Collapsed tetragonal phase and superconductivity of $BaFe_2As_2$ under high pressure

Walter Uhoya, Andrew Stemshorn, Georgiy Tsoi, and Yogesh K. Vohra
Department of Physics, University of Alabama at Birmingham (UAB), Birmingham, Alabama 35294, USA

Athena S. Sefat and Brian C. Sales
Oak Ridge National Laboratory (ORNL), Oak Ridge, Tennessee 37831, USA

Kevin M. Hope
Department of Biology, Chemistry, and Mathematics, University of Montevallo, Montevallo, Alabama 35115, USA

Samuel T. Weir
Lawrence Livermore National Laboratory (LLNL), Mail Stop L-041, Livermore, California 94550, USA
(Received 22 July 2010; revised manuscript received 9 September 2010; published 27 October 2010)

High pressure x-ray diffraction and electrical resistance measurements have been carried out on $BaFe_2As_2$ to a pressure of 35 GPa and temperature of 10 K using a synchrotron source and designer diamond anvils. At ambient temperature, a phase transition from the tetragonal phase to a collapsed tetragonal (CT) phase is observed at 17 GPa under nonhydrostatic conditions as compared to 22 GPa under hydrostatic conditions. The superconducting transition temperature increases rapidly with pressure up to 34 K at 1 GPa and decreases gradually with a further increase in pressure. Our results suggest that T_C falls below 10 K in the pressure range of 16–30 GPa, where CT phase is expected to be stable under high-pressure and low-temperature conditions.

DOI: 10.1103/PhysRevB.82.144118 PACS number(s): 62.50.−p, 74.62.Fj, 64.70.K−

The recent discovery of superconductivity in iron arsenide compounds with layered FeAs planes[1–4] has lead to extensive experimental and theoretical research on these materials in the field of high-pressure physics since application of pressure can tune the ground state of the system without introducing the disorder effects that can be induced by chemical substitutions. Among these new superconductors, the 122 compounds, AFe_2As_2 (A=alkaline-earth or rare-earth metals Ca, Sr, Ba, and Eu) having $ThCr_2Si_2$-type crystal structure stand out for their ease of growth as high-quality, homogeneous and stoichiometric, large single crystals. Also, additional interest in these 122 materials is because of the possible overlap of superconducting and antiferromagnetic phases. In particular, structural and magnetic phase transitions have been extensively investigated at ambient pressure in $BaFe_2As_2$ (Refs. 4–6) occurring at ~140 K. This transition is attributed to a spin-density wave (SDW) and a crystallographic phase transition from a tetragonal phase ($I4/mmm$) to an orthorhombic phase ($Fmmm$). The SDW transition is suppressed by either application of high pressure or chemical substitution, for example, K for Ba or Co for Fe, resulting in the appearance of superconductivity.[3,5,6] Similar observations have been made on $CaFe_2As_2$, $SrFe_2As_2$, and $EuFe_2As_2$.[7,8] Structural distortions and pressure inhomogeneity has been studied in $BaFe_2As_2$ and uniaxial stress has been reported to strongly suppress structural and SDW ordering, resulting in superconductivity at lower pressures.[9]

The present study is motivated by the occurrence of superconductivity under high pressure in $BaFe_2As_2$ and its correlation to the compression of the tetragonal (T) lattice and the occurrence of a collapsed tetragonal (CT) phase under high pressures. The compression behavior of $BaFe_2As_2$ has been studied up to 22 GPa at ambient temperature and anisotropic compression effects have been documented.[10] The first- and second-order phase transitions with strong and extremely anisotropic changes in the lattice parameters have been observed in the $ThCr_2Si_2$-structure-type compounds.[11] Also, a nonmagnetic CT phase has been documented in $CaFe_2As_2$ at 0.24 GPa and 50 K.[12] The occurrence of structural/magnetic transitions and superconductivity under different hydrostatic/nonhydrostatic conditions have been reported in $BaFe_2As_2$ single crystals.[9,13,14] Compression effect of the lattice parameters of the layered 122 compound $EuFe_2As_2$ has been extensively studied at 300 K and a T to CT reported at 8 GPa, where anomalous compression behavior reaches a maximum.[15] It is of interest to explore the occurrence of this collapsed tetragonal structure under pressure in other 122 materials and establish a correlation between superconductivity and pressure regions, where anomalous compressibility effects have been observed. The occurrence of a phase transition to a CT structure has been recently reported in $BaFe_2As_2$ at 22 GPa at 300 K and 26 GPa at 33 K under hydrostatic medium in a helium pressure medium.[16] Therefore, we have carried out detailed structural studies of $BaFe_2As_2$ under high pressures to 35 GPa at ambient temperature using image plate x-ray diffraction at a synchrotron source. The results are expressed in terms of pressure-induced anomalous compression effects, structural transformation, and equations of state. We correlate the compression behavior of $BaFe_2As_2$ with our superconductivity measurements in a similar pressure range down to 10 K.

The single-crystal samples of $BaFe_2As_2$ were grown out of a FeAs flux, as described in reference.[5] The single-crystal sample was ground and loaded in a diamond-anvil cell for the high-pressure x-ray diffraction experiments. The tetragonal crystal structure of $BaFe_2As_2$ is identified as $ThCr_2Si_2$-type with Ba atoms at 2a position (0, 0, 0), Fe atoms at 4d positions (0, 1/2, 1/4) and (1/2, 0, 1/4), As atoms at 4e position (0, 0, z) and (0, 0, $-z$). The structural parameter z=0.3545 has been obtained from Rietveld refinement of

 ©2010 The American Physical Society

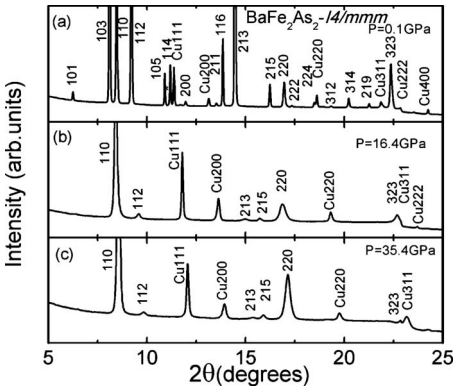

FIG. 1. The integrated x-ray diffraction profiles for $BaFe_2As_2$ at various pressures at ambient temperature using a x-ray wavelength $\lambda=0.413$ Å. (a) Diffraction pattern at a low pressure of 0.1 GPa. (b) Diffraction pattern at 16.4 GPa showing anomalous compression effects discussed in the text. (c) Diffraction pattern at the highest pressure of 35.4 GPa showing stability of the tetragonal phase. The Cu pressure marker diffraction peaks are present in all spectra.

x-ray diffraction data.[4] The high-pressure x-ray diffraction experiments were carried out at the beamline 16-ID-D, HP-CAT, Advanced Photon Source, Argonne National Laboratory. An angle dispersive technique with an image-plate area detector was employed using an x-ray wavelength $\lambda=0.413$ Å. The high-pressure sample to image plate detector distance was set to 382.9 mm. In x-ray diffraction experiments, an internal copper pressure standard was employed for the calibration of pressure.[17] The Birch Murnaghan equation,[18] shown below, was fitted to the available equation of state data on the copper pressure standard.[17]

$$P = 3B_0 f_E (1+2f_E)^{5/2}\left\{1+\frac{3}{2}(B'-4)f_E\right\} \quad (1)$$

where B_o is the bulk modulus, B' is the first derivative of bulk modulus at ambient pressure, and V_0 is the ambient pressure volume. The fitted values for copper pressure standard are $B_0=121.6$ GPa, $B'=5.583$, and $V_0=11.815$ Å^3/atom.

The parameter f_E is related to volume compression and is described below

$$f_E = \frac{\left[\left(\frac{V_o}{V}\right)^{2/3}-1\right]}{2}. \quad (2)$$

Figure 1 shows the integrated x-ray diffraction profiles for $BaFe_2As_2$ obtained at various pressures from the image-plate diffraction studies using a wavelength $\lambda=0.413$ Å. The image plate x-ray diffraction patterns were recorded with a focused x-ray beam of 5 μm$\times$8 μm on an 80 μm diameter $BaFe_2As_2$ sample mixed with copper pressure marker. The use of a focused x-ray beam allows us to collect high-quality x-ray diffraction patterns that are little affected by the inhomogeneous pressure conditions over the sample. We did not employ any pressure transmitting medium so the present studies can be regarded as nonhydrostatic where the uniaxial stress component is limited by the sample shear strength at high pressures. The geometrical constraints in our diamond-anvil cell device allowed x-ray diffraction data to be obtained to 2θ below 26°. Figure 1(a) shows the x-ray diffraction pattern at 0.1 GPa with the $BaFe_2As_2$ sample in the $I4/mmm$ phase and the copper pressure marker in the face-centered-cubic (fcc) phase. The diffraction peaks are labeled by their respective (hkl) values corresponding to crystallographic planes with Miller indices h, k, and l. The tetragonal phase of $BaFe_2As_2$ is characterized by the (101), (103), (110), (112), (200), (211), (204), (213), (220), and (323) diffraction peaks. The fcc phase of copper is characterized by the (111), (200), (220), (311), and (222) diffraction peaks. The measured volume of copper by x-ray diffraction was used to calculate sample pressure from the equation of state given by Eq. (1). Our x-ray diffraction studies at ambient conditions showed a single phase sample of $BaFe_2As_2$ with lattice parameters consistent with $a=3.9635(5)$ Å, $c=13.022(2)$ Å, and axial ratio $c/a=3.285$.[5] The measured lattice parameters at 0.1 GPa are $a=3.961\pm0.002$ Å and $c=13.004\pm0.006$ Å, with $c/a=3.283$. Figure 1(b) shows the x-ray diffraction spectrum at a pressure of 16.4 GPa with lattice parameters $a=3.9842\pm0.002$ Å and $c=10.595\pm0.006$ Å. Comparing 16.4 GPa with 0.1 GPa data, the (112), (213), and (323) diffraction peaks shift to higher diffraction angles or lower interplanar spacing with increasing pressure while the (110) and (220) move to higher interplanar spacing [Figs. 1(a) and 1(b)]. This is a clear evidence of the anomalous compression of the tetragonal lattice. This is in contrast to normal compression behavior which shows a uniform decrease in all dimensions of the unit cell. These observations agree very well with the previous high pressure studies of polycrystalline $BaFe_2As_2$ under quasihydrostatic condition in a helium pressure medium, where the a axis was found to increase with compression while the c axis decreased at T-CT structural transition and the CT phase in the $I4/mmm$ tetragonal structure was found to be stable up to 56 GPa at 300 K.[16] Another important point to note is that (213) and (220) diffraction peaks remain single peaks without any evidence of splitting and hence there is no evidence of a tetragonal to orthorhombic phase transformation at high pressures, which is noted at low temperatures,[3,4,6] and also at ambient temperatures and high pressures.[10] Figure 1(c) shows that the phase remains tetragonal until the highest pressure of 35.4 GPa with lattice parameters $a=3.9149\pm0.002$ Å and $c=9.809\pm0.006$ Å. The compression of the tetragonal lattice between 16.4 and 35.4 GPa can be considered normal as all diffraction peaks move to higher angles or lower interplanar d spacings as can be seen by comparing Figs. 1(b) and 1(c). Also note that as pressure is increased beyond 16 GPa, the reflections such as (101), (112), (211), and (200) progressively decreases in intensity and the structure looks simpler. The decrease in intensity of tetragonal peaks such as (101) and the simplicity of high-pressure phase could mean that the body centering and hence the $I4/mmm$ symmetry may not exist anymore. However, apart from the reflections from the fcc phase of copper, all the other observed Bragg peaks were clearly indexed with $I4/mmm$ tetragonal structure up to the highest static pressure of 35 GPa. Our attempts to fit the highest pressure phase with other possible structure such as hexagonal NiAs phase

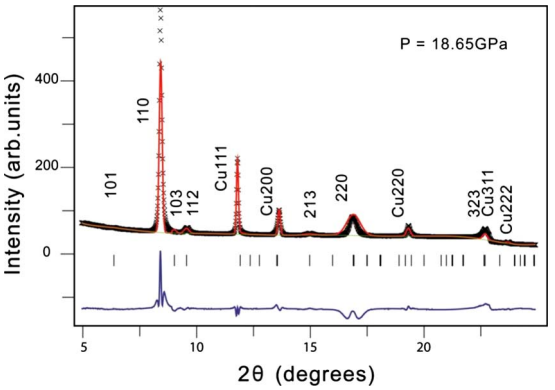

FIG. 2. (Color online) Observed x-ray diffraction pattern (solid x symbols), Rietveld fit (solid curve in the top spectrum), and difference between observed and calculated profiles (bottom curve) obtained after Rietveld refinement of $BaFe_2As_2$ at 300 K and 18.7 GPa (space group $I4/mmm$). The refinement was done using GSAS Rietveld package with a March-Dollase preferred orientation along the (110) plane.

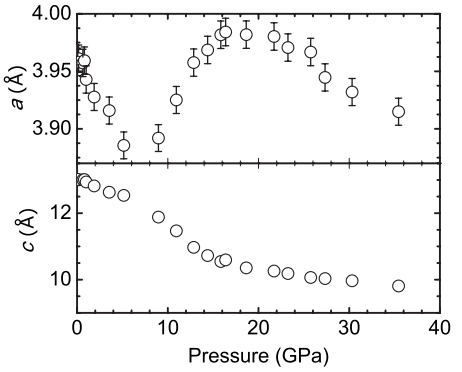

FIG. 3. The measured a and c lattice parameters for the tetragonal phase of $BaFe_2As_2$ as a function of pressure. A negative compressibility is observed for the a axis and a maximum is observed at 16.4 GPa. The c axis shows a rapid decrease with increasing pressure till 16.4 GPa and a normal decrease with further increase in pressure. The error bars for c are less than the symbol size.

did not provide any satisfactory fits. The decrease in intensity of (hkl) with nonzero l values can be explained by pressure-induced texturing effect where the c axis of the grains tends to orient along the load axis of the diamond-anvil cell.

To elucidate the preferred orientation effects, we have performed Rietveld refinements of an x-diffraction pattern from the sample at 18.7 GPa, just after the T-CT phase transition (Fig. 2). This provides further evidence that the observed change in intensity at higher pressures can be explained by the preferred orientation in the sample and is not due to any structural phase transition. The difference between the observed x-ray diffraction pattern and Rietveld refined spectrum is reasonable considering a simple orientation model where c axis is aligned along the load axis of the diamond-anvil cell (Fig. 2). The Rietveld refinements were performed using GSAS Rietveld package with a March-Dollase preferred orientation along the (110) plane.[19] The refinement treated the (110) plane as a preferred orientation. If there were no preferred orientation then all refraction planes would be represented with the same weight of 1.00. The refinement gave (110) plane a weight of 0.26, this would demonstrate a definite preferred orientation for the system.

Figure 3 shows the measured lattice parameters a and c as a function of pressure exhibiting anomalous compression effects. Below 5.2 GPa, both a and c lattice parameters shrink with increasing pressure. Then the structure follows abnormal behavior whereby a increases with increasing pressure with a peak at a pressure of 16.4 GPa. A further increase in pressure beyond 16.4 GPa, results in a decrease in a axis and a normal compression behavior that continues until the highest pressure of 35 GPa. This negative compressibility of a axis is a very intriguing feature of $BaFe_2As_2$ compression. The c lattice parameter shows a rapid decrease with increasing pressure between 9 and 16 GPa, and a normal decrease with further increase in pressure to 35 GPa. These observations show that continuous second-order phase transition starts between ~5 and ~9 GPa. At ~16.4 GPa, $BaFe_2As_2$ completely transforms to a high-pressure collapse tetragonal structure within the same space group but with a larger a and smaller c lattice parameters. The observed changes of a axis and c axis of $BaFe_2As_2$ between 5 and 16 GPa and normalized to values at 16 GPa are −15.5% for c axis, +2.5% for a axis, −11.1% for volume and −17.6% for c/a. These changes are extremely anisotropic and are similar to those of $LaFe_2P_2$ between 4 and 9 GPa and $EuFe_2P_2$ between 2 and 9 GPa.[11]

Figure 4 shows the measured axial ratio (c/a) as a function of pressure to 35 GPa at ambient temperature. The axial ratio (c/a) shows a rapid decrease with increasing pressure till 16 GPa and a gradual decrease above this pressure. In fact, the c/a ratio variation as a function of pressure can be divided into two linear regions and the fits for the two linear regions are shown in Fig. 3 and described below

$$c/a = 3.510 - 0.054P, \quad 5 \leq P \leq 16 \text{ GPa}, \tag{3}$$

$$c/a = 2.692 - 0.005P, \quad 18 \leq P \leq 35 \text{ GPa}. \tag{4}$$

The intersection of the two linear regions as described by Eqs. (3) and (4) defines the phase transition from the ambient

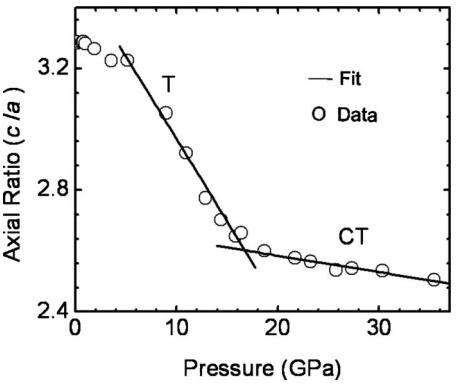

FIG. 4. The measured axial ratio (c/a) for the tetragonal phase of $BaFe_2As_2$ as a function of pressure to 35 GPa. The linear fits for the two phases, i.e., the T phase and the CT phase are described in the text. The transition between the two phases occurs at 16.7 GPa at ambient temperature.

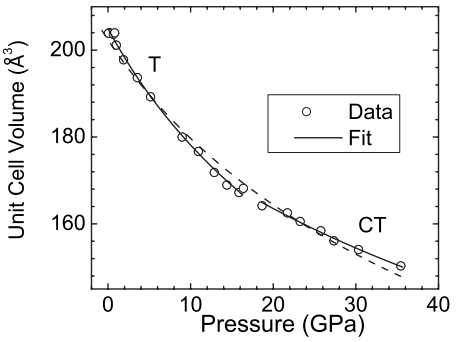

FIG. 5. The measured equation of state data for the tetragonal phase of $BaFe_2As_2$ as a function of pressure to 35 GPa. The solid curves are the Birch-Murnaghan equation of state fit to the two phases, i.e., the T phase (low-pressure region) and the CT phase (high-pressure region). The continuous dash line shows a single Birch-Murnaghan equation of state fit for the entire low- and high-pressure data combined. The fit parameters are summarized in Table I. The transition between the two phases occurs at 16.7 GPa at ambient temperature.

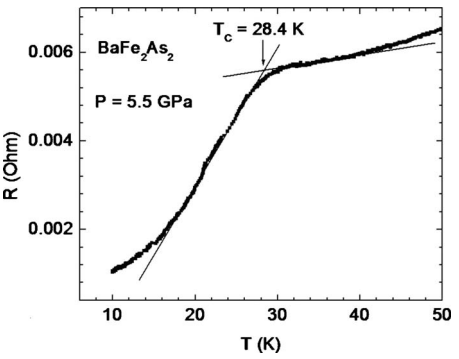

FIG. 6. The measured electrical resistance of $BaFe_2As_2$ sample as a function of temperature at 5.5 GPa indicating onset of superconductivity at 28.4 K.

pressure T phase to the so-called CT phase. This phase transition is defined by the present experiments to occur near 16.7 GPa at ambient temperature. A further x-ray diffraction study at low temperature would be needed to follow this phase boundary to low temperatures.

Figure 5 shows the measured pressure-volume (P-V) curve or equation of state for $BaFe_2As_2$ to 35 GPa at ambient temperature. Also shown are the Birch-Murnaghan equation of state fits as described by Eq. (1). The fit parameters for the tetragonal and collapsed tetragonal phases are summarized in Table I. The fitted ambient pressure volume (V_0) is 205.0 Å^3 for the T phase and 190.4 Å^3 for the CT phase, indicating that a hypothetical CT phase at ambient pressure has a density that is 7.1% higher than the T phase (Table I). The measured equation of state shows considerable stiffening at the tetragonal to collapsed tetragonal phase transition as evidenced by the change in slope of the volume-pressure curve at 16.7 GPa as shown in Fig. 5. The fitted value of Bulk Modulus B_0=57.7 GPa for the T phase and B_0=104.4 GPa for the CT phase at ambient pressure. This comparison shows that the T phase of $BaFe_2As_2$ is more compressible than a hypothetical CT phase at ambient pressure by a factor of 1.8. The dashed curve in Fig. 5 shows a single Birch-Murnaghan equation of state fit for the entire low- and high-pressure P-V data combined. The single fit deviates quite significantly from the measured P-V data in comparison to the two fit obtained when high- and low-pressure regions are fitted separately. The single-fit parameters are also included in Table I for comparison purposes.

The superconducting transition (T_C) measurements have been carried out using four probe electrical resistance measurements in a designer diamond anvil as described in an earlier publication.[20] In this study, no pressure medium was used and hence the reported superconducting transition temperatures correspond to a nonhydrostatic case. The continuous phase transition observed in $BaFe_2As_2$ may be closely related to the behavior of T_C observed experimentally under different pressures. Figure 6 shows the electrical resistance as a function of temperature at a pressure of 5.5 GPa indicating onset of superconductivity at 28.4 K. Figure 7 shows the measured onset of T_C as a function of pressure up to 30 GPa and down to 10 K. T_C increases to a maximum temperature of 34 K at a pressure of 1.0 GPa and then decreases monotonically with increase in pressure from 1.0 to 8.3 GPa. The pressure dependence of the superconducting transition temperature for single crystalline $BaFe_2As_2$ shown in Fig. 7 under nonhydrostatic conditions is also compared to the data reported by Mani *et al.*[21] to a maximum pressure of 7 GPa in a solid steatite pressure-transmitting medium and a good agreement is obtained. Figure 7 shows that T_C variation as a function of P can be described by a second-order polynomial equation shown below

$$T_C(\mathrm{K}) = (34.93 \pm 0.71) - (0.99 \pm 0.32)P - (0.06 \pm 0.03)P^2,$$

$$1.0 \leq P \leq 8.3 \ \mathrm{GPa}. \qquad (5)$$

The solid line is the polynomial fit to experimental T_C (P) data in Fig. 7 and it suggests that T_C decreases rapidly in the region where anomalous compressibility effects are observed in the *a* axis. The extrapolation of the second order polynomial fit described above suggests that T_C approaches 0 K at 17 GPa and a nonsuperconducting state is achieved above

TABLE I. Equation of state parameters for $BaFe_2As_2$ sample in the T phase and CT phase at ambient temperature.

Phase	Unit-cell volume (V_0) ambient conditions	Bulk modulus (B_0)	Pressure derivative of bulk modulus (B')
T $0 < P < 16.7$ GPa	204.97 ± 0.60 Å^3	57.7 ± 1.5 GPa	4.0 ± 0.4
CT 17 GPa $< P < 35$ GPa	190.43 ± 2.23 Å^3	104.4 ± 8.2 GPa	3.1 ± 0.6
Combined T-CT phases $0 < P < 35$ GPa	202.4 ± 1.30 Å^3	70.32 ± 2.9 GPa	5.6 ± 0.5

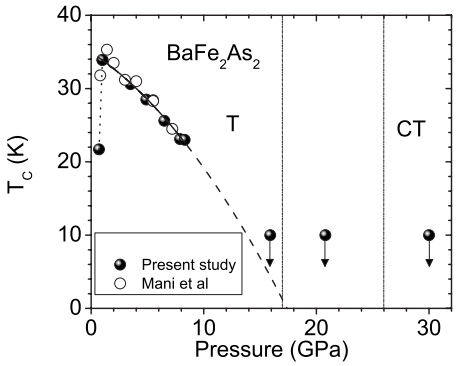

FIG. 7. The measured superconducting transition temperature as a function of pressure for $BaFe_2As_2$ as obtained by electrical resistivity measurements using a diamond anvil cell. T_C increases to a maximum temperature of 34 K at a pressure of 1.0 GPa and then decreases monotonically with decrease in pressure between 1.0 and 8.3 GPa. The T_C below 10 K could not be determined because the lowest temperature limit in this study is 10 K and graphical points with down-arrow indicate that T_C is likely to be below this temperature. The solid curve shows a second-order polynomial fit to data and it is described in the text. The region between the vertical lines at 17 and 26 GPa represent the pressure range over which T-CT transition would seem likely to occur at low temperatures. Our data is in excellent agreement with an earlier study of Mani *et al.* (Ref. 21) to 7 GPa.

this pressure, however, direct measurements below 10 K and in the pressure range of 15–30 GPa are needed to support this extrapolation. It is interesting to note that our measured structural x-ray diffraction data also shows a transition from tetragonal to a collapsed tetragonal phase at around 17 GPa at 300 K. Previous powder synchrotron diffraction experiment on polycrystalline sample shows that this transition occurs at 22 GPa at 300 K and 26 GPa at 33 K using a helium pressure medium.[16] The phase transition from tetragonal to collapsed tetragonal phase seems to be sensitive to the magnitude of uniaxial stresses that may explain the scatter in transition pressure from 17 to 22 GPa at ambient temperature. The region between vertical lines at 17 and 26 GPa, therefore, represent the pressure range over which this structural transition would seem likely to occur at low temperatures. The T_C values for higher pressures could not be determined because the lowest temperature possible using our experimental set up in this study is only 10 K and graphical points with down-pointing arrows in Fig. 7 indicates that onset of T_C is suppressed to below this temperature limit of 10 K in the pressure region where T-CT phase transition occur. Additional low-temperature experiments below 10 K are needed to precisely pinpoint the disappearance of superconductivity and correlate it to stability of the CT phase. In contrast, this observation differ from that reported in $EuFe_2As_2$ (Ref. 15) in which superconducting transition temperature was observed to be enhanced in the region where anomalous compression is robust, reaching a maximum around T-CT phase transition region. However, europium 122 compounds have a pressure induced valence transition from Eu^{2+} to Eu^{3+} in the pressure range of anomalous compression that needs to be accounted for in making comparison with alkaline-earth metal compounds.

In conclusion, we have carried out a superconductivity study under high pressure using four probe electrical resistance measurements, with designer diamond anvils up to 30 GPa and down to 10 K, and high pressure powder x-ray diffractions measurements of $BaFe_2As_2$ to 35 GPa at ambient temperature using a synchrotron source. The image plate x-ray diffraction studies reveal an anomalous compression effect of the *a* axis and a structural phase transition from the normal T phase to the CT at 16.7 GPa and ambient temperature. The equation of state for the T phase and CT phase show distinct bulk moduli and pressure derivatives of Bulk Moduli. At ambient pressure, an extrapolated CT phase has a density that is 7.1% higher as compared to the T phase under similar conditions. The superconducting transition (T_C) is marked by a decrease in electrical resistance as a function of temperature. The measured value of T_C shows a second order polynomial decrease from a maximum of 34 K at 1.0 GPa down to 23 K at 8.3 GPa and is extrapolated to 0K at 17 GPa, which is the same pressure region where the sample changes from normal tetragonal phase to collapsed tetragonal phase. Our high-pressure studies have shown anomalous compressibility effects, the presence of a possible collapsed tetragonal phase, and superconducting properties that are correlated with its compression behavior. We suggest that the anomalous compressibility effect observed in the lattice parameter for $BaFe_2As_2$ under pressure may be a common effect among the 122 compounds of the type AFe_2As_2 (A = divalent alkaline-earth or rare-earth metal) having the $ThCr_2Si_2$-type crystal structure and may be related to observed superconductivity in $BaFe_2As_2$. Additional systematic theoretical and experimental studies of structural phase transitions and superconductivity in $BaFe_2As_2$ under hydrostatic and nonhydrostatic pressure conditions and lower temperatures are required to clearly establish a correlation between transition pressure, superconductivity, and crystal structure.

Walter Uhoya acknowledges support from the Carnegie/Department of Energy (DOE) Alliance Center (CDAC) under Grant No. DE-FC52-08NA28554. Andrew Stemshorn acknowledges support from the Department of Education under Grant No. P200A090143. Research at ORNL is sponsored by the Materials Sciences and Engineering Division, Office of Basic Energy Sciences, U.S. Department of Energy. We greatly acknowledge discussions with Michael A. McGuire, and David Mandrus at ORNL. Portions of this work were performed at HPCAT (Sector 16), Advanced Photon Source (APS), Argonne National Laboratory.

[1] Y. Kamihara, T. Watanabe, M. Hirano, and H. Hosono, J. Am. Chem. Soc. **130**, 3296 (2008).
[2] H. Takahashi, K. Igawa, K. Arii, Y. Kamihara, M. Hirano, and H. Hosono, Nature (London) **453**, 376 (2008).
[3] M. Rotter, M. Tegel, and D. Johrendt, Phys. Rev. Lett. **101**, 107006 (2008).
[4] M. Rotter, M. Tegel, D. Johrendt, I. Schellenberg, W. Hermes, and R. Pöttgen, Phys. Rev. B **78**, 020503(R) (2008).
[5] A. S. Sefat, R. Jin, M. A. McGuire, B. C. Sales, D. J. Singh, and D. Mandrus, Phys. Rev. Lett. **101**, 117004 (2008).
[6] P. L. Alireza, J. Gillett, Y. T. Chris Ko, S. E. Sebastian, and G. G. Lorezarich, J. Phys.: Condens. Matter **21**, 012208 (2009).
[7] M. S. Torikachvili, S. L. Bud'ko, N. Ni, and P. C. Canfield, Phys. Rev. Lett. **101**, 057006 (2008).
[8] T. Park, E. Park, H. Lee, T. Klimczuk, E. D. Bauer, F. Ronning, and J. D. Thompson, J. Phys.: Condens. Matter **20**, 322204 (2008).
[9] W. J. Duncan, O. P. Welzel, C. Harrison, X. F. Wang, X. H. Chen, F. M. Grosche, and P. G. Niklowitz, J. Phys.: Condens. Matter **22**, 052201 (2010).
[10] J.-E. Jørgensen, J. Staun Olsen, and L. Gerward, Solid State Commun. **149**, 1161 (2009).
[11] C. Huhnt, W. Schlabitz, A. Wurth, A. Mewis, and M. Reehuis, Physica B **252**, 44 (1998).
[12] A. I. Goldman, A. Kreyssig, K. Prokes, D. K. Pratt, D. N. Argyriou, J. W. Lynn, S. Nandi, S. A. J. Kimber, Y. Chen, Y. B. Lee, G. Samolyuk, J. B. Leao, S. J. Poulton, S. L. Bud'ko, N. Ni, P. C. Canfield, B. N. Harmon, and R. J. McQueeney, Phys. Rev. B **79**, 024513 (2009).
[13] K. Matsubayashi, N. Katayama, K. Ohgushi, A. Yamada, K. Munakata, T. Matsumoto, and Y. Uwatoko, J. Phys. Soc. Jpn. **78**, 073706 (2009).
[14] F. Ishikawa, N. Eguchi, M. Kodama, K. Fujimaki, M. Einaga, A. Ohmura, A. Nakayama, A. Mitsuda, and Y. Yamada, Phys. Rev. B **79**, 172506 (2009).
[15] W. Uhoya, G. Tsoi1, Y. K Vohra, M. A. McGuire, A. S. Sefat, B. C Sales, D. Mandrus, and S. T. Weir, J. Phys.: Condens. Matter **22**, 292202 (2010).
[16] R. Mittal, S. K. Mishra, S. L. Chaplot, S. V. Ovsyannikov, E. Greenberg, and D. M. Trots, L. Dubronvinsky, Y. Su, T. Brueckel, S. Matsuishi, H. Hosono, and G. Garbarino, arXiv:1007.2320v1 (unpublished).
[17] N. Velisavljevic and Y. K. Vohra, High Press. Res. **24**, 295 (2004).
[18] F. Birch, Phys. Rev. **71**, 809 (1947).
[19] A. C. Larson and R. B. Von Dreele, Los Alamos National Laboratory Report No. LAUR 86–748, 2004 (unpublished).
[20] G. Tsoi, A. Stemshorn, Yogesh K. Vohra, Phillip M. Wu, F. C. Hsu, Y. L. Huang, M. K. Wu, K. W. Yeh, and Samuel T. Weir, J. Phys.: Condens. Matter **21**, 232201 (2009).
[21] A. Mani, N. Ghosh, S. Paulraj, A. Bharathi, and C. S. Sundar, EPL **87**, 17004 (2009).